JOURNAL OF QUATERNARY SCIENCE (2017) **32**(1) 63–79 ISSN 0267-8179. DOI: 10.1002/jqs.2924

JQS Journal of Quaternary Science QRA Quaternary Research Association

# The sedimentary history of the inner-alpine Inn Valley, Austria: extending the Baumkirchen type section further back in time with new drilling

**SAMUEL BARRETT,[1]* REINHARD STARNBERGER,[1] RIK TJALLINGII,[2] ACHIM BRAUER[2] and CHRISTOPH SPÖTL[1]**

[1]Institute of Geology, University of Innsbruck, Innrain 52, Innsbruck, 6020, Austria

[2]Section 5.2: Climate Dynamics and Landscape Evolution, GFZ German Research Centre for Geosciences, Potsdam, Germany

Received 2 November 2015; Revised 9 November 2016; Accepted 13 November 2016

ABSTRACT: The Baumkirchen clay pit near Innsbruck, western Austria, is a well-known site in Alpine Quaternary stratigraphy. Lacustrine sediments from the last glacial cycle from within the Alps provide a unique opportunity to investigate the regional palaeoclimate. Recent drilling has extended the known sequence to a total length of at least 250 m consisting of almost entirely well-laminated clayey silt. Luminescence dating identified two lake sequences, separated by a hiatus of ca. 7000–15 000 years. Lake phase 1 spans the period ca. 77–55 ka, i.e. from about Marine Isotope Stage (MIS) 5/4 to the MIS 4/3 transition. Lake phase 2 extends from mid- to late MIS 3 between ca. 45 and 33 ka. Down-core X-ray fluorescence core scanning confirmed the presence of the lake phases in the sediment composition, suggesting different sediment sources and/or transport mechanisms during these two intervals. A unique section of exotic, angular, silt matrix-supported gravel at the top of lake phase 1 is interpreted as ice-rafted debris. Luminescence dating constrains this layer to ca. 55 ka, thus providing the first evidence of a late MIS 4 or early MIS 3 ice advance confined to the interior of the Eastern Alps. A conceptual model of the sedimentary history of the valley is presented. Copyright © 2017 John Wiley & Sons, Ltd.

KEYWORDS: Alps; luminescence dating; palaeolake; Würmian; XRF.

## Introduction

The Baumkirchen clay pit east of Innsbruck, Austria, is a classic site in Alpine Quaternary stratigraphy. The long sequence of fine-grained sediments (the Baumkirchener Bändertone) has been known since the late 19th century (Blaas, 1890; Fliri, 1999), and the hypothesis of a large palaeo-lake was originally put forward by Penck (1890) and discussed by Penck and Brückner (1909) and Ampferer (1908). The discovery of (radiocarbon-) datable plant macrofossils in 1969 led to a surge of research, most notably into the sedimentology (Köhler and Resch, 1973), pollen (Bortenschlager and Bortenschlager, 1978), micro- and macrofossils (summary in Fliri, 1973) and chronostratigraphy (Fliri, 1970, 1976; Fliri *et al.*, 1971, 1972). The known sequence comprises banded clayey silts exposed in the clay pit near the villages of Baumkirchen and Fritzens, which transition up into sand and then gravel in the surrounding area. This transition is the type locality for the boundary between the Middle and Upper Würmian in the Eastern Alps (Chaline and Jerz, 1984). These sediments are part of the larger Gnadenwald terrace, extending along the northern edge of the Inn Valley from the edge of the Hall fan in the west and to the outflow of the Vomperloch gorge in the east over a distance of ca. 10 km. The terrace rises around 250 m above the present height of the river Inn and is capped by Last Glacial Maximum (LGM) till (Fliri, 1975; Spötl *et al.*, 2014).

Two main models for lacustrine sedimentation have been proposed for the Baumkirchen sequence: (i) the 'fjord model' of a large and rather deep lake filling the Inn Valley for many kilometres dammed by a sediment wedge near the confluence between the Inn and Ziller valleys (originally by Penck and Brückner, 1909 and more recently by Sarnthein and Spötl, 2012), and (ii) the 'alluvial fan model' of several smaller and shallower lakes dammed by a series of aggrading alluvial fans (originally by Ampferer, 1908 and later refined by van Husen, 1983a).

Re-dating of the original radiocarbon samples by accelerator mass spectrometry (AMS) techniques by Spötl *et al.* (2013) places the Bänderton in the Baumkirchen clay pit in late Marine Isotope Stage 3 (MIS 3) with ages of ca. 35 cal ka BP. Greenland ice core (e.g. North Greenland Ice Core Project members, 2004) and Atlantic marine oxygen isotope records (e.g. Bond *et al.*, 1999) indicate that MIS 3 was dominated by a series of abrupt, high-magnitude climate variations known as Dansgaard Oeschger (DO) events. Oxygen isotope speleothem records indicate that these abrupt DO events were not limited to the North Atlantic but are also strongly expressed in the climate of the Alpine region (Moseley *et al.*, 2014). Huntley *et al.* (2003) reviewed European terrestrial pollen datasets for this period, which recorded distinct warm and cool phases, but which did not reach either fully glacial or interglacial conditions. Alpine terrestrial records for this period are scarce (e.g. Heiri *et al.*, 2014); however, several sites in the foreland indicate unstable conditions with marked stadials and interstadials. The Füramoos pollen record from south-west Germany revealed three, albeit very poorly dated, interstadials during early to mid-MIS 3 (up to a hiatus at ca. 40 ka) (Müller *et al.*, 2003). The pollen record from the 'mammoth peat' at Niederweningen in the Swiss alpine foreland indicates a cold to warm transition in early MIS 3 (Anselmetti *et al.*, 2010), while coleopteran assemblages from lignites at Gossau (eastern Switzerland) indicate distinctly cooler periods where trees would barely be able to grow (Jost-Stauffer *et al.*, 2005).

A significant outstanding question is whether there were any major glacial advances in the Alps to the foreland during the last glacial period (Würmian) before the LGM. Ivy-Ochs *et al.* (2008) and Preusser (2004) discussed evidence of an MIS 4 lowland advance in the Western Alps (although the evidence is only indirect from pollen or presumed

*Correspondence to: Samuel Barrett, as above.
E-mail: samuel.barrett@student.uibk.ac.at

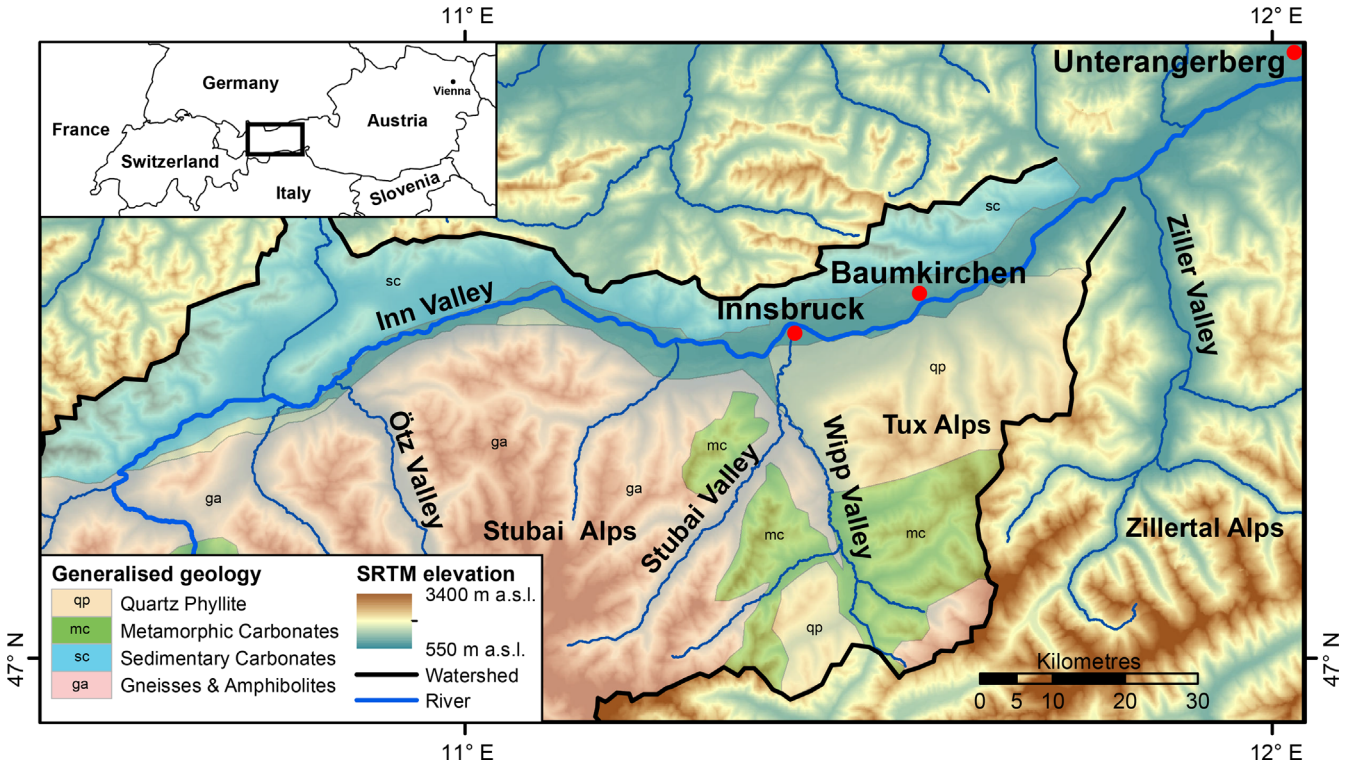


**Figure 1.** Overview showing the study area topography (SRTM 30-m resolution), major rivers and Alpine regions. The generalized geology of the catchment area is shown by dominant rock type (source: Geological Survey of Austria).

fluvioglacial sediments) and noted the absence of evidence from the Eastern Alps, except for a possible site in the Allgäu region (Link and Preusser, 2005). This discrepancy is added to by the indication of ice-free conditions in the Eastern Alps at Unterangerberg (Fig. 1) in the lower Inn Valley downstream from Baumkirchen (Starnberger *et al.*, 2013a). Despite the lack of evidence for an advance and its extent, various models have been proposed to explain the mismatch, notably a crucial difference in the height and thus accumulation potential between the Western and Eastern Alps, the increase in continentality in an eastward direction, and different atmospheric circulation patterns (e.g. Preusser, 2004).

### *Luminescence dating of lake sediments*

Key to advancing our understanding of early MIS 3 and older palaeoclimate and palaeoenvironments is the reliable dating of these sediments. Plant macro remains are very rare in most alpine sediment successions of this age range and radiocarbon dates older than ca. 40 ka are associated with increasingly large uncertainties (e.g. Brauer *et al.*, 2014). Optical dating techniques are therefore commonly the only possibility to provide a robust, albeit not high-precision chronological framework for such fine-grained sediments. In the European Alps, first attempts to date Pleistocene waterlain deposits using optically stimulated luminescence (OSL) were made by Preusser (1999a,b) in the Swiss Alpine foreland and by Link and Preusser (2005) and Klasen *et al.* (2007) in the northern Alpine foreland and the interior of the Eastern Alps, respectively. A well-studied site in this respect is Niederweningen, near Zurich, Switzerland, where quartz and feldspar were used to reconstruct the climatic and sedimentation history there from MIS 3 back to MIS 6 (Anselmetti *et al.*, 2010; Lowick and Preusser, 2011; Dehnert *et al.*, 2012). Furthermore, Lowick *et al.* (2012) highlighted the importance of considering both bleaching and anomalous fading when working with fine-grained lacustrine samples from mountain areas to ensure that the latter is not overprinted by the former.

At Baumkirchen, the first luminescence dating approach was undertaken by Klasen *et al.* (2007), who reported very low quartz luminescence sensitivity but good feldspar characteristics, and thus recommended future studies on this mineral at this site. Also in the Inn Valley of Austria, but further east, Starnberger *et al.* (2013a,b) studied several Early and Middle Last Glacial lake phases from a number of sediment cores using polymineral fine-grained lake sediment samples. They applied a post-infrared stimulated single aliquot regenerative dose (pIRIR-SAR) protocol and concluded that the pIRIR was unsuitable for dating these samples, because it largely overestimated independent age control, presumably due to incomplete bleaching. Fading-uncorrected infrared stimulated luminescence (IRSL) data, however, agreed with calibrated radiocarbon ages.

The emergence of new analytical techniques in Quaternary science provides powerful tools to further study underinvestigated palaeoclimate records. The significant advances in luminescence dating during the last decade and the emergence of high-resolution X-ray fluorescence (XRF) core scanning in particular motivated the renewed investigation of the Baumkirchen sequence. Due to the sparseness of pre-LGM inner-Alpine climate records, this study, which is based on new scientific drill cores, aims to provide new palaeoclimate information about the response of the Alpine environment during the last glacial cycle, specifically regarding DO events and MIS 4 glacier fluctuations.

## Materials and methods

### *Study area*

The Baumkirchen site (670 m a.s.l., 47.306°N, 11.569°E) is located ca. 12 km east of Innsbruck, Austria, in the E–W-trending central Inn Valley, one of the largest valleys in the Alps (Fig. 1). The location north of the main Alpine divide presently has a humid continental climate. The area to the north is part of the Northern Calcareous Alps (NCA), consisting largely of limestone and dolomite, with only a few small

valleys draining to the south into the Inn Valley. To the south and west of Innsbruck the Ötz, Stubai and Wipp Valleys drain the Ötztal, Stubai and Tux Alps. These mountains are dominated by gneisses and schists of the Ötztal-Stubai crystalline complex, although there are also areas of metamorphic carbonates including dolomites and calc-schists. The Tux and Zillertal Alps to the south of Baumkirchen are drained by the Ziller and a series of smaller valleys south of Baumkirchen. This area is mainly composed of the Innsbruck Quartzphyllite, with a small area of carbonate-bearing meta-sediments (Tarntal Mesozoic; Pfiffner, 2014).

## *Scientific drilling*

Four overlapping holes at two sites were drilled during the summers of 2010 and 2013, and 11.5-cm inner diameter liner cores (1.5-m sections) totalling ca. 330 m were recovered. The first were collected at the eastern edge of the abandoned and partly re-filled Baumkirchen clay pit, and the second in the forest nearby (Fig. 2). The cores were split, prepared and logged, and are stored at the University of Innsbruck.

Several Brenner Railway Company (BEG) cores (positions in Fig. 2), drilled between 1995 and 1999, were used to provide additional information about the internal sediment fill of the Gnadenwald terrace. The existing drilling logs from the BEG were simplified based on dominant grain size to gravel, sand and silt/clay with a fourth category of silty matrix-supported gravel. Several surface outcrops shown in Fig. 2 were also investigated. Samples for luminescence dating were taken from outcrops at Bärenbach and in the Schotterwerk III gravel pit (Table S1).

## *Grain size analysis*

Gravels from a short section of the Baumkirchen cores and the Schotterwerk III exposure were wet-sieved to >32, 16–32, 8–16 and <8 mm grain size fractions. These sub-samples were further sorted by angularity and basic petrography (limestone, dolomite and different types of crystalline rocks).

## *Elemental composition*

The chemical composition of the fine-grained lacustrine sediments from the Baumkirchen cores was analysed using an ITRAX XRF core scanner at the GFZ Potsdam, Germany. In total, 146 m of core was scanned to cover the most significant parts of the composite profile. Sediment cores were selected based on the core description and comprise a near-complete 96-m-long section and approximately 50 m distributed throughout the remaining ca. 150 m of the sequence (Fig. 3).

The XRF scanner was equipped with a Mo X-ray source operating at 30 kV and 40 mA with measurement times of 5 or 10 s. Most of the sediment was analysed at 1-mm resolution and a small number of finely laminated sections were investigated at 0.2-mm resolution.

The elemental composition acquired by XRF core scanning comprises count rates (cps) of nine major elements (Ca, Si, K, Ti, Mn, Fe, Zn, Rb, Sr). To minimize the effects of changes in physical sediment properties and sample geometry, element intensities are converted into element ratios and centred-log ratios (e.g. $Ca_{clr}$) (Weltje and Tjallingii, 2008).

## *Luminescence dating*

### *Sample preparation*

For dating purposes, fine- and coarse-grained sediment samples from drill cores and outcrops were collected either from undisturbed core sections or from freshly cleaned outcrops, the latter using stainless steel cylinders. In core

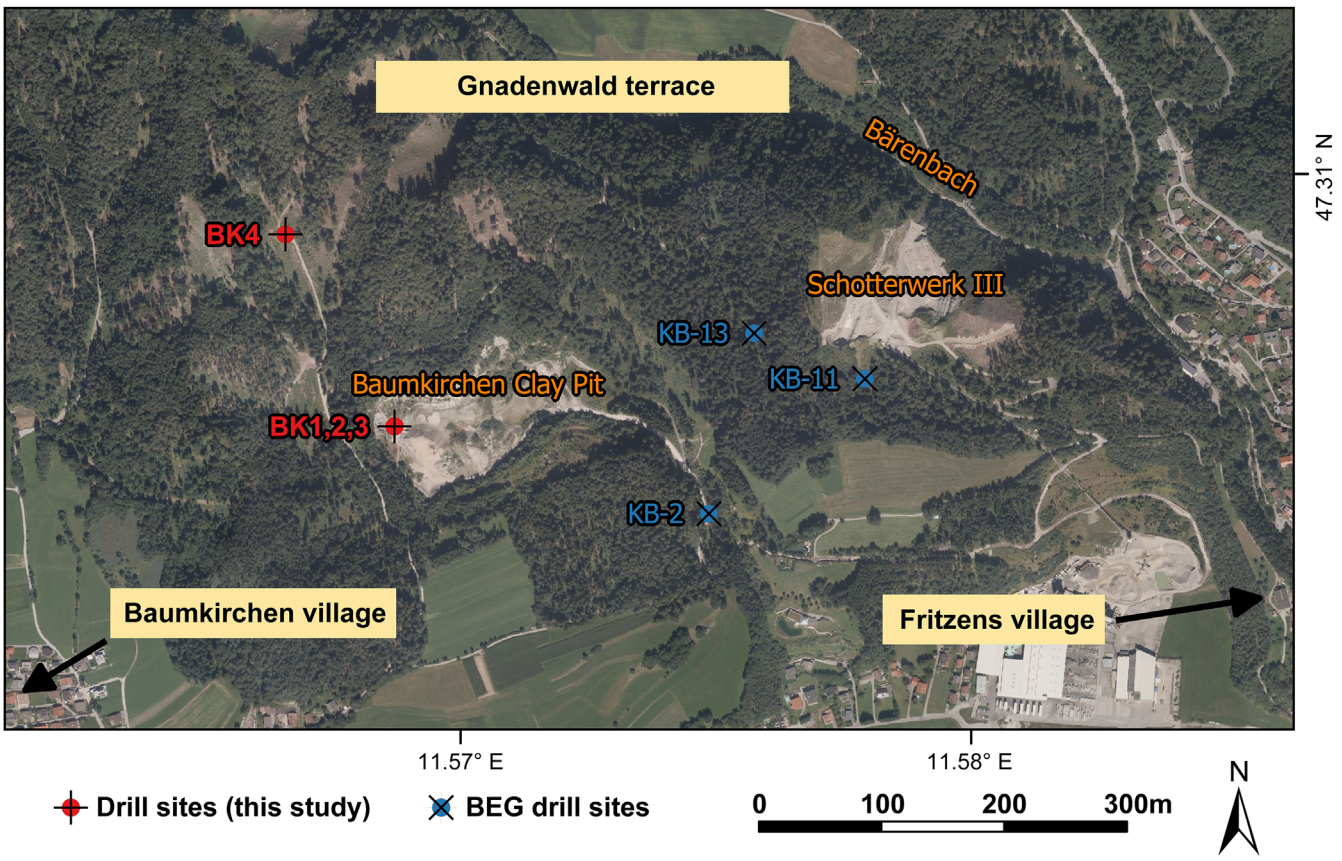


**Figure 2.** Overview of the location and geographical context of the important sites on the Gnadenwald terrace near the Baumkirchen clay pit, including surface exposures and drilling locations (this study in red, BEG in blue).

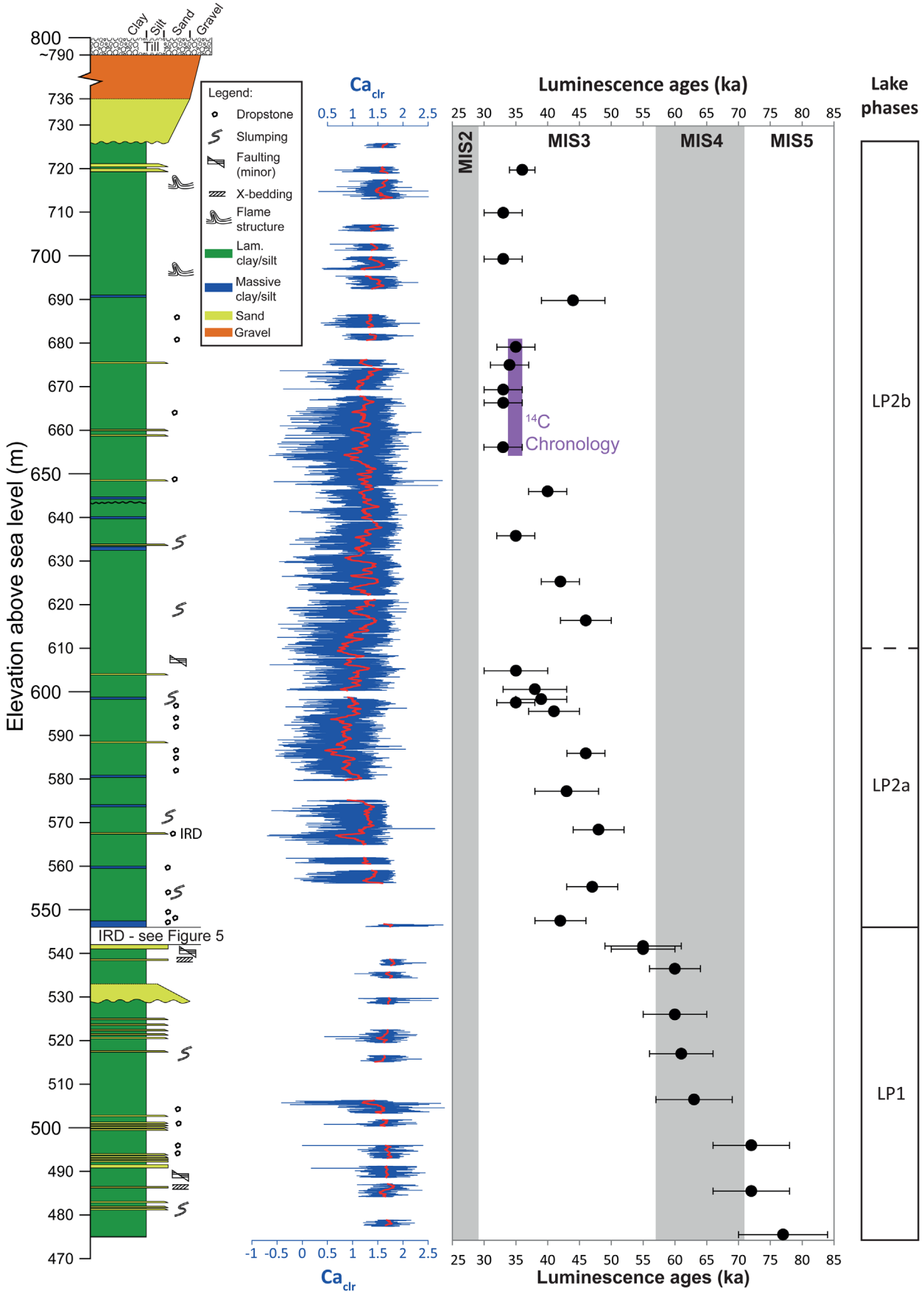


**Figure 3.** Simplified sedimentary log of the Baumkirchen sequence showing the downcore XRF $Ca_{clr}$ record (blue, no averaging; red, 20-cm moving average) and the luminescence ages with uncertainties. The violet bar indicates the radiocarbon-dated interval (Spötl *et al.*, 2013). Indicated faults have offsets of <5 cm. Indicated slumping is on sub metre scale except around 630 m a.s.l. where the disturbed sediment extends over several metres.

sections where XRF core scanning was performed, samples for luminescence dating were taken from the split core half that was not used for XRF measurement. All further analyses were made under subdued red light conditions in the Innsbruck luminescence laboratory. The outermost, light-exposed parts of the samples were removed, and the remaining material was chemically treated with hydrochloric acid (10%, v/v) and hydrogen peroxide (10%, v/v) to remove carbonates and organics, respectively. Samples were washed with distilled water after every treatment step. Fine-grain (4–11 μm) polymineral samples were prepared by settling (using sodium oxalate) and repeated washing and centrifuging following Frechen *et al.* (1996). Fine-grain measurement aliquots were produced by mounting the sediment on 9.7-mm-diameter aluminium discs using acetone (1 mg per aliquot). Coarse-grain K-feldspar samples were prepared by extracting the 180–212 μm sand fraction by dry sieving and subsequent heavy liquid density separation using LST Fastfloat (2.58 g $cm^{-3}$). For these samples, small measurement aliquots (1 mm in diameter) were produced by mounting the grains onto stainless steel discs (9.7 mm in diameter) using silicone oil spray.

*Measurement protocol*

Luminescence measurements were carried out by using a Risø TL/OSL DA-15 or Risø TL/OSL DA-20 Reader equipped with calibrated $^{90}Sr/^{90}Y$ beta sources delivering ca. 0.08 or ca. 0.10 Gy $s^{-1}$, respectively. The feldspar signal was stimulated using infrared light diodes at 870 nm and recorded in the blue–violet spectrum using a Schott BG39/Corning 7–59 filter combination. For all measurements, heating was at 5 °C $s^{-1}$ in a nitrogen atmosphere. A measurement error of 1.6% was derived experimentally and assumed for all equivalent dose ($D_e$) estimations. For dating, rejection criteria for individual aliquots were: (i) a detected signal of less than three times the background, (ii) a recycling ratio not between 0.9 and 1.1, (iii) a recuperation above 5% or (iv) a test dose error above 10%.

For $D_e$ estimations, we used a modified post-IR IRSL SAR protocol which includes an elevated temperature measurement step (Thomsen *et al.*, 2008; Thiel *et al.*, 2011). This was done to make use of a signal which is potentially less prone to anomalous fading and has been successfully applied before to date similar deposits (Starnberger *et al.*, 2013b) (Table 1). Before applying this protocol, a suitable preheat (PH) temperature was evaluated by performing a PH plateau test using a standard IRSL SAR protocol (i.e. stimulation at 50 °C only), where a PH plateau could be identified between 220 and 280 °C (Supplementary Material, Fig. S1). For all subsequent measurements, preheating was then set at 250 °C. The IRSL at 50 °C from the pIRIR protocol ($IRSL_{50/225}$) and the post-IR IRSL at 225 °C ($pIRIR_{225}$) were each recorded for 300 s and integrated over the first 5 s, with a background taken from the last 50 s (Table 1). To improve measurement reproducibility, test dose measurement preheat was held at the same temperature used for the natural and regeneration doses for all IR-luminescence measurements (Blair *et al.*, 2005).

**Table 1.** Modified IRSL-SAR protocol used for equivalent dose estimations.

| Step | Treatment | Observed |
|---|---|---|
| 1 | Give dose | |
| 2 | Preheat (250 °C for 60 s) | |
| 3 | IR stimulation (50 °C for 300 s) | $L_n/L_x$ ($IRSL_{50/225}$) |
| 4 | IR stimulation (225 °C for 300 s) | $L_n/L_x$ ($pIRIR_{225}$) |
| 5 | Give test dose | |
| 6 | Preheat (250 °C for 60 s) | |
| 7 | IR stimulation (50 °C for 300 s) | $T_n/T_x$ ($IRSL_{50/225}$) |
| 8 | IR stimulation (225 °C for 300 s) | $T_n/T_x$ ($pIRIR_{225}$) |
| 9 | Return to 1 | |

*Dose rate*

For determination of the dose rate-relevant elements, inductively coupled plasma mass spectrometry (ICP-MS after Preusser and Kasper, 2001) was applied to all core samples and BK3 outcrop samples, whereas thick source alpha (Daybreak 583 alpha counter) and beta counting (Risø GM25-5 beta counter) were applied to the other outcrop samples (i.e. from Bärenbach). To check for potential inconsistencies of these two different approaches, some of the samples were measured in both ways and the resulting dose rate values were consistent. The external beta and gamma dose rates were calculated using the conversion factors of Adamiec and Aitken (1998). The effect of alpha irradiation was considered with an a-value of $0.07 \pm 0.02$ following Klasen *et al.* (2007). Cosmic dose rate values were obtained using the equations given by Prescott and Hutton (1994). Where available, present-day water content values were used for dose-rate calculations (Absam, Bärenbach and Baumkirchen outcrops; BK3 and BK4 cores; some BK1 and BK2 core samples). In all other cases, a water content of 25% was assumed. To take past changes of moisture into account, a water content error of 10% was used for all samples. The relevant data are presented in Table S1. The ADELE software (Kulig, 2005) was used to calculate luminescence ages.

## Results

### *Sedimentology and stratigraphy*

The four overlapping drill cores recovered from the Baumkirchen clay pit reveal a sequence of at least 250 m of laminated lacustrine sediments (down to ca. 474 m a.s.l.), even though the bottom of the sequence was not reached. The overlapping cores were correlated by matching distinctive layers or groups of layers, allowing a composite record to be obtained (Fig. 3). Logging revealed that the sequence is almost entirely well laminated on a millimetre–centimetre scale and that the appearance of the lamination changes only subtly, of which three representative examples are shown in Fig. 4. Laminae are distinct by colour and/or grain size and can be split roughly into 'background' (BG) sediment and coarser 'medium silt-fine sand' (mS-S) layers. Background sediments mainly consist of fine to very fine silts with a clay matrix that are interrupted by coarser layers which lack the clay matrix and contain medium silt to fine sand. There is, however, a continuum between these categories, and sediment which is not strongly BG or mS-S is also shown in Fig. 4 labelled as 'Intermediate'. The sediment throughout the drilled sequence is very similar to that previously described in the quarry itself (Fliri, 1973). Dropstones are found occasionally throughout the sequence (Fig. 3) and with the exception of the short interval around 545 m a.s.l., all are angular carbonates or sandstone from the NCA. Minor slumping was observed in several places, the most significant of which extends over several metres around 630 m a.s.l. and features repeated groups of recognizable laminae which are sometimes overturned (Fig. 3).

Among the >250 m of almost entirely laminated clayey silt of the sequence in the Baumkirchen cores, logging revealed a short interval of chaotic, unlaminated silts with

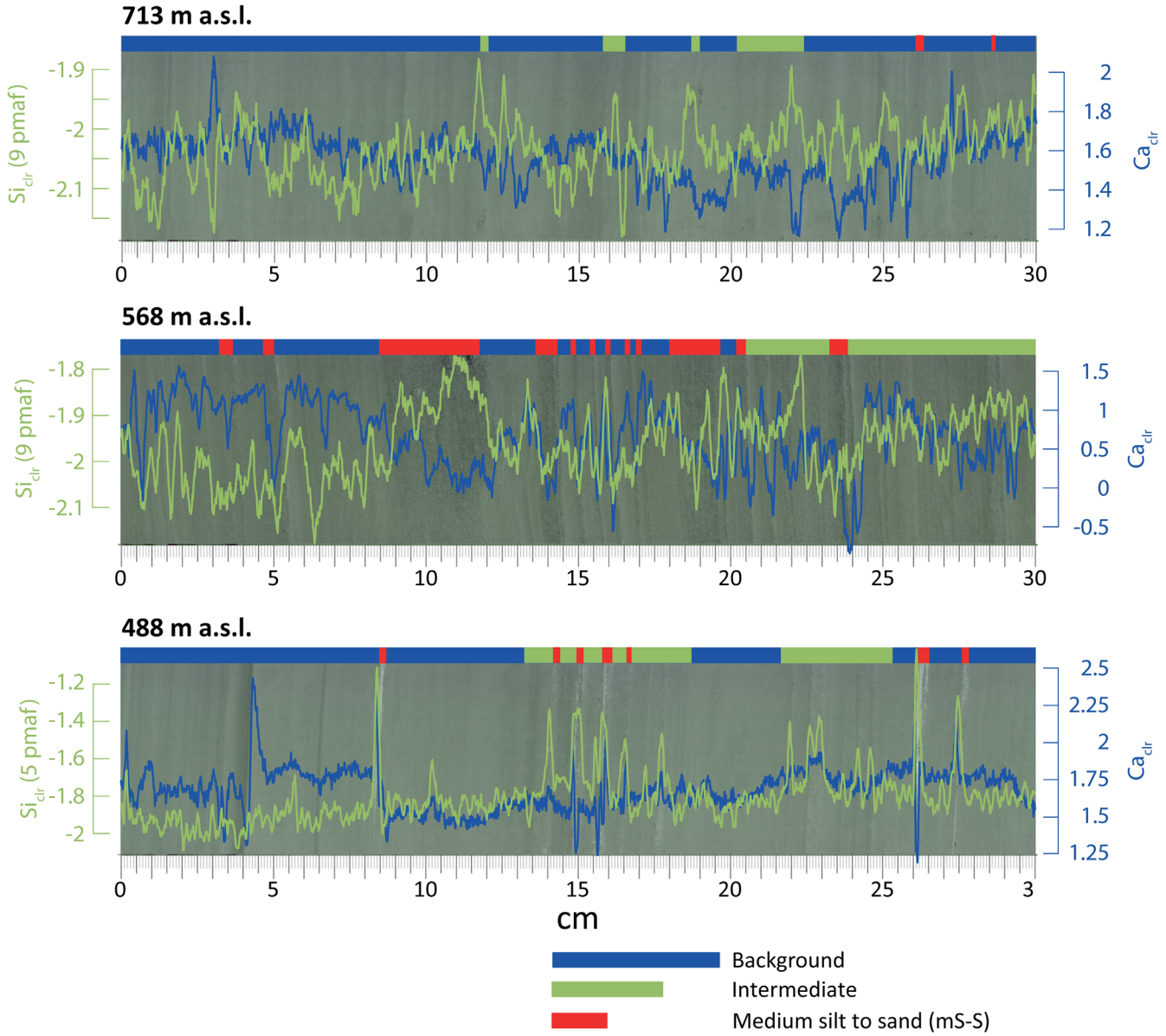


**Figure 4.** Examples of the similar appearance of the Baumkirchen banded silt from three different elevations with the $Si_{clr}$ and $Ca_{clr}$ XRF data overlain. The lamina classifications for the intervals are shown – see text. X pmaf = 'X point moving average filter'.

sandy intervals, disturbed in places, with several layers rich in dropstones (gravel-sized clasts in silty clay matrix) at around 545 m a.s.l. The largest of these was one ca. 80-cm-thick gravel layer (Fig. 5). The clasts are of diverse petrography (a mix of non-metamorphic carbonate and crystalline rocks – Fig. 5), are mostly angular, and include a significant component of gneisses from the Ötztal–Stubai complex (20+ km to the south-west – Fig. 1). This interval is hereafter referred to as the ice-rafted debris (IRD) layer, because its origin is attributed to ice rafting (see Discussion). By contrast, gravel from the nearby Schotterwerk III gravel pit was dominantly rounded low-grade metamorphic clasts with a dominant component from the nearby (ca. 5+ km to the south) Innsbruck Quartzphyllite.

## *Elemental composition*

As log-ratios of element intensities are linearly related to log-ratios of absolute element concentrations (Weltje and Tjallingii, 2008; Weltje *et al.*, 2015), the relative variations in the proportions of Si and Ca reveal changes in the abundance of carbonates (assuming no major contribution from plagioclases) versus silicates. The patterns in the XRF element data shown in Fig. 4 clearly follow visible changes in sediment character seen in the core images. In the lowest section around 488 m a.s.l., the pattern of Si clearly follows the mS-S layers – all of which are high in Si and thus silicates. In contrast, in the 568 m a.s.l. section, some of the mS-S layers are high in Si while others are low. While Ca is also high in some of the mS-S layers in the 488 m a.s.l. section, it is typically rather low in similar layers in the other two sections. The Ca values in the BG and the sediment in general are lower in the middle 568 m a.s.l. section than the others (Fig. 3). The Ca curve can be split into two sections, the lower section below 550 m a.s.l. with high values and low variance, and the longer upper section above with lower Ca values but a higher variance with a gradual decrease in variance from ca. 670 m a.s.l. towards the top of the sequence.

## *Luminescence properties*

Representative regeneration dose–response growth curves and natural signal decay curves of the IRSL, $IRSL_{50/225}$ and $pIRIR_{225}$

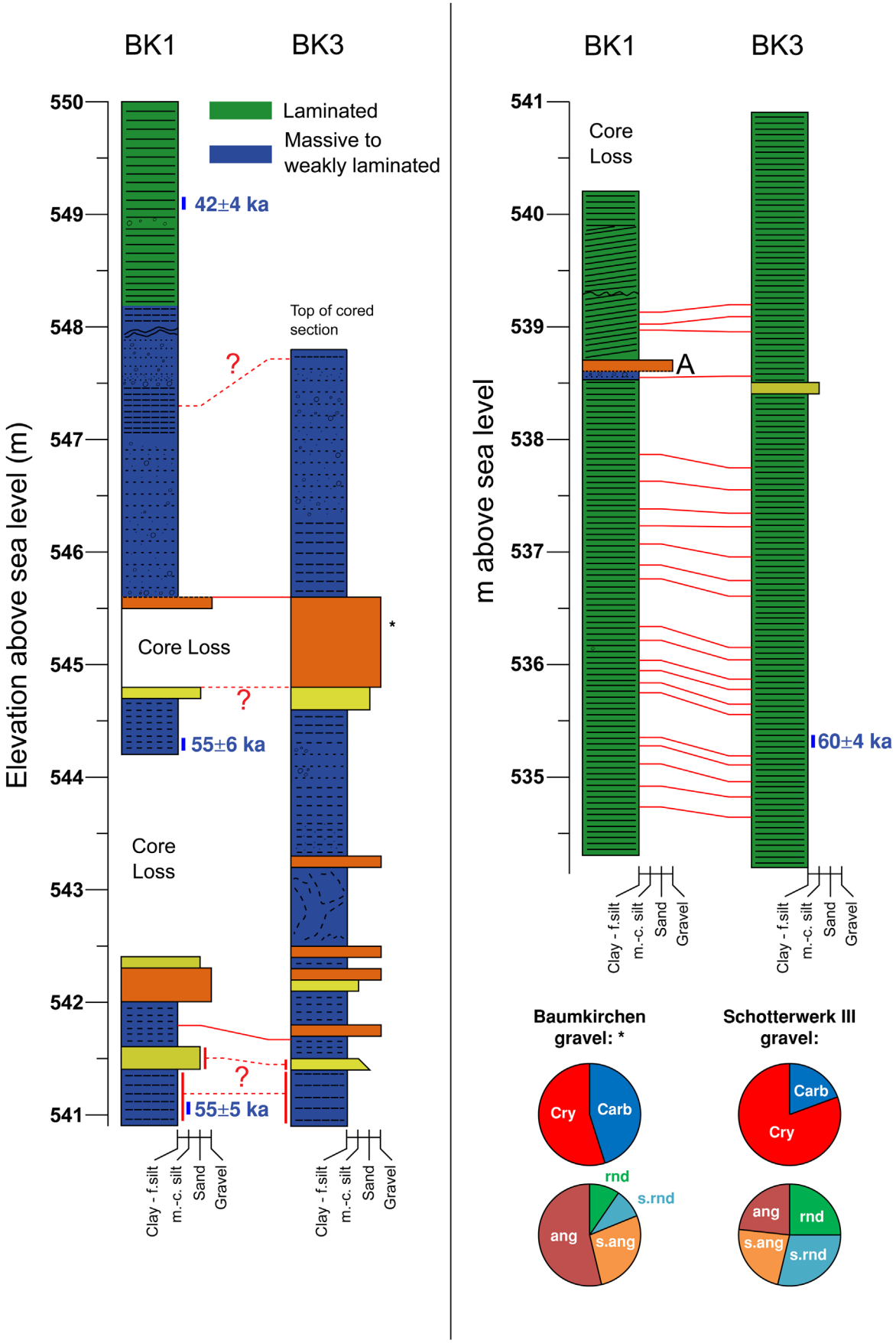


**Figure 5.** Sedimentary log of the IRD section in the Baumkirchen cores with luminescence ages, and gravel composition in comparison with Schotterwerk III. Carb = carbonate, Cry = crystalline, ang = angular + very angular, s.ang = subangular, s.rnd = subrounded, rnd = rounded + very rounded.

signals for an aliquot of sample BK2-208A are shown in Fig. 6. The conventional $IRSL_{50}$ and the $IRSL_{50/225}$ and $pIRIR_{225}$ are compared to detect the potential impact of the pIRIR stimulation step on the equivalent doses of the conventional $IRSL_{50}$. The results show that the equivalent doses as well as the signal intensity show no significant difference between the conventional $IRSL_{50}$ and the $IRSL_{50/225}$, i.e. the one from the post-IR IRSL SAR protocol (Fig. 6). Therefore, the $IRSL_{50/225}$ signal is regarded as reliable to be used for age determination. The dose–response curves for high laboratory doses also show that $2D_0$ values which represent 85% of the signal saturation (Wintle and Murray, 2006) are ca. 450 Gy for the IRSL, ca. 390 Gy for the $IRSL_{50/225}$ and ~400 Gy for the $pIRIR_{225}$. The equivalent doses of all these three signals lie clearly below this value (Table 2), which means that from the saturation point of view they are generally all useful for dating. When compared to the $IRSL_{50}$ and $IRSL_{50/225}$ signals, the $pIRIR_{225}$ signal results in distinctively higher $L_x/T_x$ values and, consequently, in a higher equivalent dose ($D_e$) (Fig. 6). This is representative for all other samples analysed in this study and may be explained either by anomalous fading of the IRSL and $IRSL_{50/225}$ signals, insufficient zeroing of the $pIRIR_{225}$ signal before last deposition, or a combination of the two. To clarify this, anomalous fading tests were carried out, and the bleaching behaviour of the different feldspar signals was investigated. This helped to identify the best suited signal for dating (in the following discussion, $IRSL_{50/225}$ is shortened to IRSL, and $pIRIR_{225}$ to pIRIR).

All samples were tested to see whether the chosen protocol was able to recover a known laboratory dose (290–370 Gy) administered to previously light-exposed and unheated sediment samples (dose recovery tests after Wallinga *et al.*, 2000; Murray and Wintle, 2003). This is an important check for the suitability of the material for luminescence dating and for the degree of signal resetting (bleaching) during exposure to natural sunlight. In the optimum case, the dose recovery test renders a measured/given dose ratio of around unity (±10%). Before the dose recovery test, residual doses were measured on 14 previously unheated aliquots from five different core samples which were exposed to sunlight for at least 5 days (Fig. 7B). These residuals (average of ~3.6 Gy for the IRSL and average of ~13.5 Gy for the pIRIR) were then subtracted from the equivalent doses from the new, previously unheated and (10 days) sunlight-bleached aliquots used for the dose recovery test. Dose recovery test results are shown in Fig. S2 for 10 samples from different depths in cores BK1 and BK3. All the IRSL results lie within the range of 0.9–1.1, which means that the previously administered dose could be successfully recovered. For the pIRIR signals all measured/given ratios are larger than one, and for three samples the values clearly exceed the threshold of 1.1. This effect might be due to the different bleaching characteristics of the respective signals as discussed below.

To further investigate the bleaching characteristics of the IRSL and pIRIR signals, a bleaching experiment with different sunlight exposure times was conducted. In total, 36 aliquots of fine-grained material from BK2-201A were exposed for between 10 s and 2 h with three aliquots for each exposure time. This experiment also gave information about the minimum time needed to reset the luminescence signal. The results from the bleaching experiment (Fig. 7A) indicate distinctively different bleaching behaviour of the two signals: while the IRSL is reduced to <5% of the natural signal after ca. 10 min, the pIRIR still carries a 10% residual dose. After 2 h, the IRSL is at ca. 2%, while the pIRIR is reduced to ca. 4%. The results of the additional residual dose tests show an average residual dose of 3.6 Gy (ca. 2% of the natural dose) for the IRSL and 13.5 Gy (ca. 6% of the natural dose) for the pIRIR, but with a larger variation for the latter. If considered in the dose recovery test, the subtraction of residual doses helps to reduce the previously too high pIRIR values to less than 1.1 in four out of five cases. These results together indicate that the IRSL signal of the samples from the Gnadenwald terrace has generally good bleaching properties and is not affected by residual doses, whereas the pIRIR bleaches distinctively more slowly and has a larger hard-to-bleach component. For the IRSL, the good bleaching characteristics also allow us to expect that fading, if present, should not be masked by incomplete bleaching when measuring the natural signal.

Anomalous fading tests were performed to check for any significant signal loss of the IRSL and post-IR IRSL signals

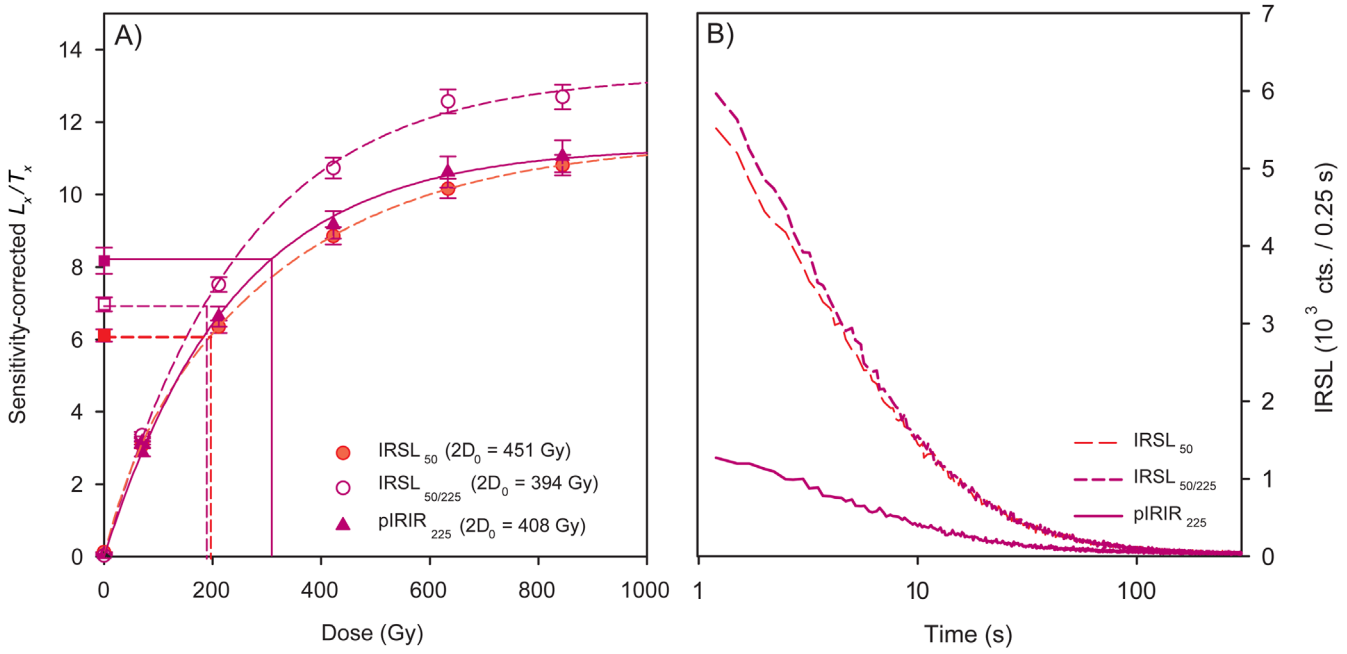


**Figure 6.** (A) Regeneration dose response and (B) natural signal decay curves for the IRSL, the $IRSL_{50/225}$ and $pIRIR_{225}$ signals of sample BK2-208A.

**Table 2.** IRSL fine-grained polymineral results from the Baumkirchen sequence, and nearby surface exposures ($n$ = number of aliquots; $D_e$ = equivalent dose; DR = environmental dose rate).

| Site/core | Sample | Elevation (m a.s.l.) | $n$ | $D_e$ IRSL (Gy) | $DR_m$ (Gy ka$^{-1}$) | IRSL age$_m$ ka) |
|---|---|---|---|---|---|---|
| Absam gravel pit outcrop | Abs2 | ca. 700 | 5 | 90 ± 5 | 2.7 ± 0.3 | 33 ± 4 |
| | Abs3 | ca. 700 | 5 | 82 ± 7 | 2.1 ± 0.2 | 36 ± 5 |
| Baumkirchen outcrop | BK00 | 675 | 8 | 217 ± 9 | 6.4 ± 0.4 | 34 ± 3 |
| Core BK2 | 201A | 669.36 | 6 | 173 ± 7 | 5.3 ± 0.3 | 33 ± 3 |
| | 208A | 666.33 | 8 | 195 ± 9 | 5.9 ± 0.3 | 33 ± 3 |
| | 215W | 656.14 | 6 | 201 ± 9 | 6.0 ± 0.4 | 33 ± 3 |
| Core BK1 | 20W | 646 | 8 | 217 ± 9 | 5.1 ± 0.2 | 40 ± 3 |
| | 27W | 635.79 | 10 | 202 ± 17 | 5.7 ± 0.3 | 35 ± 3 |
| | 34W | 625.31 | 10 | 231 ± 8 | 5.3 ± 0.2 | 42 ± 3 |
| | 40W | 616.39 | 8 | 241 ± 13 | 5.1 ± 0.3 | 46 ± 4 |
| | 47A | 604.83 | 8 | 213 ± 24 | 5.7 ± 0.3 | 35 ± 5 |
| | 50A | 600.6 | 9 | 208 ± 8 | 5.3 ± 0.3 | 38 ± 5 |
| | 52W-1 | 597.54 | 7 | 216 ± 6 | 5.2 ± 0.2 | 35 ± 3 |
| | 52W-2 | 598.35 | 10 | 216 ± 13 | 5.6 ± 0.2 | 39 ± 4 |
| | 54W | 595.55 | 10 | 229 ± 16 | 5.3 ± 0.3 | 41 ± 4 |
| | 60W | 585.85 | 10 | 281 ± 10 | 6.1 ± 0.3 | 46 ± 4 |
| | 66W | 577.2 | 10 | 248 ± 20 | 5.4 ± 0.3 | 43 ± 5 |
| | 73W | 568.42 | 9 | 240 ± 16 | 5.5 ± 0.3 | 48 ± 4 |
| | 81W | 555.28 | 9 | 257 ± 32 | 5.7 ± 0.3 | 47 ± 4 |
| | 85W | 550.5 | 5 | 246 ± 16 | 5.7 ± 0.3 | 42 ± 4 |
| | 87W | 547.5 | 5 | 422 ± 36 | 4.3 ± 0.3 | 98 ± 13 |
| | 91W | 541.7 | 6 | 284 ± 13 | 5.0 ± 0.3 | 55 ± 6 |
| | 92W | 541 | 8 | 285 ± 10 | 5.1 ± 0.3 | 55 ± 5 |
| Core BK3 | 09W | 536.5 | 8 | 312 ± 11 | 5.2 ± 0.3 | 60 ± 4 |
| | 16W | 526 | 7 | 297 ± 3 | 5.0 ± 0.3 | 60 ± 5 |
| | 22W | 517 | 6 | 312 ± 13 | 5.1 ± 0.3 | 61 ± 5 |
| | 29W | 506.5 | 9 | 347 ± 21 | 5.5 ± 0.3 | 63 ± 6 |
| | 36W | 496 | 7 | 386 ± 10 | 5.4 ± 0.2 | 72 ± 6 |
| | 43W | 485.5 | 7 | 358 ± 11 | 4.9 ± 0.3 | 72 ± 6 |
| | 50W | 475.6 | 5 | 392 ± 15 | 5.2 ± 0.3 | 77 ± 7 |
| Core BK4 | 21W | 719.7 | 8 | 192 ± 5 | 5.3 ± 0.3 | 36 ± 2 |
| | 27W | 709.9 | 8 | 165 ± 15 | 5.0 ± 0.3 | 33 ± 3 |
| | 34W | 699.3 | 10 | 180 ± 13 | 5.4 ± 0.3 | 33 ± 3 |
| | 41W | 689.8 | 10 | 236 ± 20 | 5.4 ± 0.3 | 44 ± 5 |
| | 48W | 679.1 | 9 | 181 ± 7 | 5.2 ± 0.3 | 35 ± 3 |
| K-KB | 02/95 | 612.3 | 5 | 208 ± 15 | 5.2 ± 0.3 | 40 ± 4 |
| | | 576.4 | 5 | 202 ± 26 | 5.4 ± 0.3 | 37 ± 5 |
| | | 550.2 | 5 | 172 ± 17 | 3.4 ± 0.2 | 51 ± 6 |
| Schotterwerk III outcrop | IIIA | 660 | 7 | 224 ± 5 | 5.8 ± 0.4 | 55 ± 5 |
| | IIIB | 660 | 7 | 245 ± 26 | 5.8 ± 0.4 | 61 ± 8 |

over different storage times. Fading tests were made on BK1 samples following Auclair *et al.* (2003), but modified by including the pIRIR measurement step into the conventional IRSL protocol (Table 1). Aliquots were repeatedly irradiated using regeneration doses (ca. 86 Gy) and test doses (ca. 6 Gy), and then preheated to 250 °C before prompt and delayed $L_x/T_x$ measurement of IRSL and pIRSL. The longest delay time between preheating and $L_x/T_x$ measurements was around 27 h. Calculations of $g$-values as a measure for the natural signal loss per decade were made following Aitken (1998). Figure 8 shows $g$-values from 23 aliquots of four samples from core BK1. Both the IRSL and pIRIR $g$-values show some scatter, but it is clear that in general the fading rates are relatively low, with an average of 2.2 ± 0.9% per decade for the IRSL and of 0.8 ± 1.1% per decade for the pIRIR signal. These values indicate that the age underestimation due to anomalous fading is relatively low in our study, which is especially true for the $pIRIR_{225}$ values which might well be laboratory artefacts (Buylaert *et al.*, 2012). As anomalous fading correction is only for the linear part of the dose–response curve, and the natural doses measured in this study are all clearly older than that, age underestimation of the true depositional age cannot be quantified. Thus, the IRSL and pIRIR ages are left un-corrected.

## *Luminescence ages*

Considering the large difference between the natural doses of the IRSL and pIRIR signals, and the relatively poor bleachability of the pIRIR signal, we conclude that the IRSL signal from the pIRIR protocol is much better suited to deliver realistic ages than the pIRIR, and that the pIRIR signal is generally affected by incomplete bleaching. The reliability of the IRSL ages can be tested by the independent age control available in the upper part of the sequence (ca. 650–680 m a.s.l). Here, radiocarbon dating of wood and other plant macro remains found ca. 50 m away from the drill site and in the same stratigraphic context resulted in calibrated radiocarbon ages of ca. 34–35 cal ka BP (Spötl *et al.*, 2013). Five luminescence samples from the drill cores correspond to this interval (BK2-215W, BK2-208A, BK2-201A, BK00 and BK4-48W). The ages determined from both the IRSL and pIRIR signals are shown along with the radiocarbon dates in Fig. 9. The IRSL ages can be seen to agree closely with the

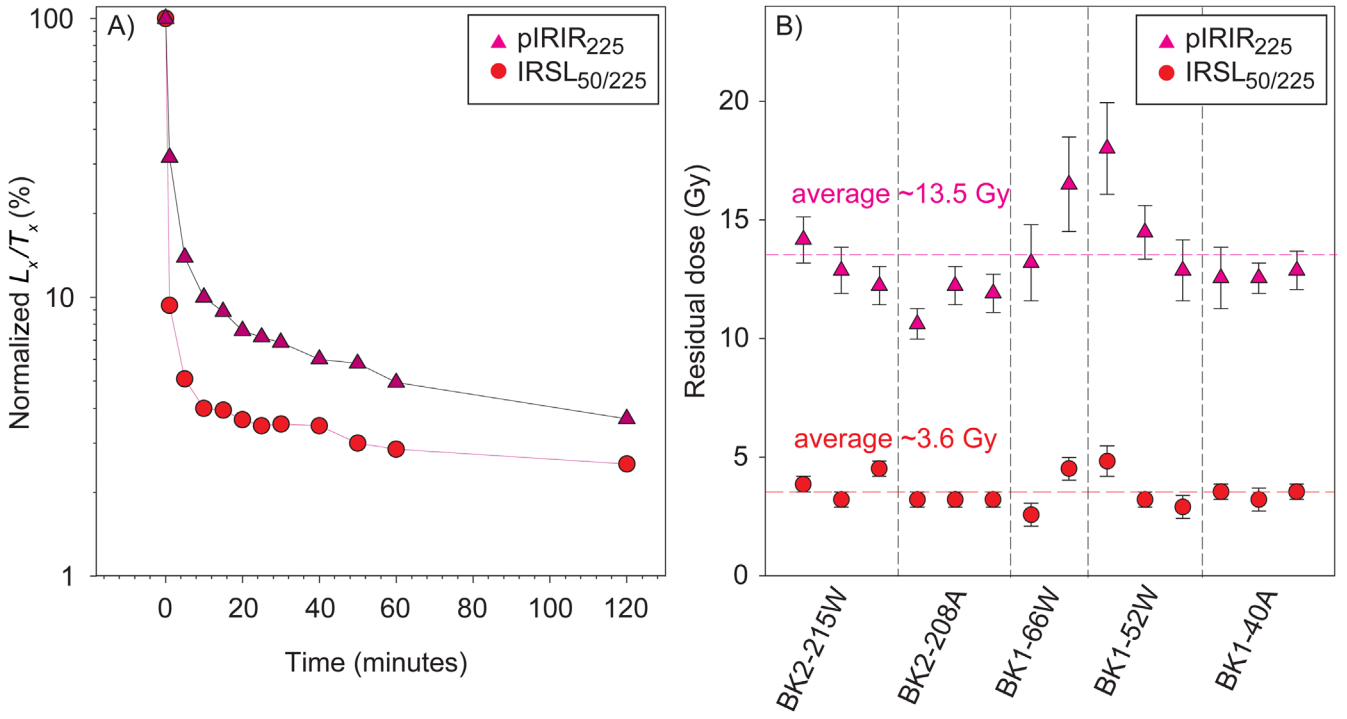


**Figure 7.** (A) Results of the bleaching experiment for the $IRSL_{50/225}$ (circles) and the $pIRIR_{225}$ (triangles) signals, with samples exposed to direct natural sunlight between 10 s and 2 h before measurement. Each data point is the average of three aliquots. (B) Residual $IRSL_{50/225}$ and $pIRIR_{225}$ doses measured on 14 aliquots from five samples of core BK1 and BK2 after 10 days of exposure to natural sunlight.

independent age control within uncertainties. In contrast, the pIRIR ages have a greater degree of scatter and are between 17 000 and 36 000 years older than the radiocarbon ages. Thus, we consider the IRSL signal more reliable for age determination. Table 2 shows the IRSL-derived ages, and all further discussion refers to these ages.

The ages from the drill cores are generally stratigraphically consistent, with the oldest ages of around 74 ka at the bottom,

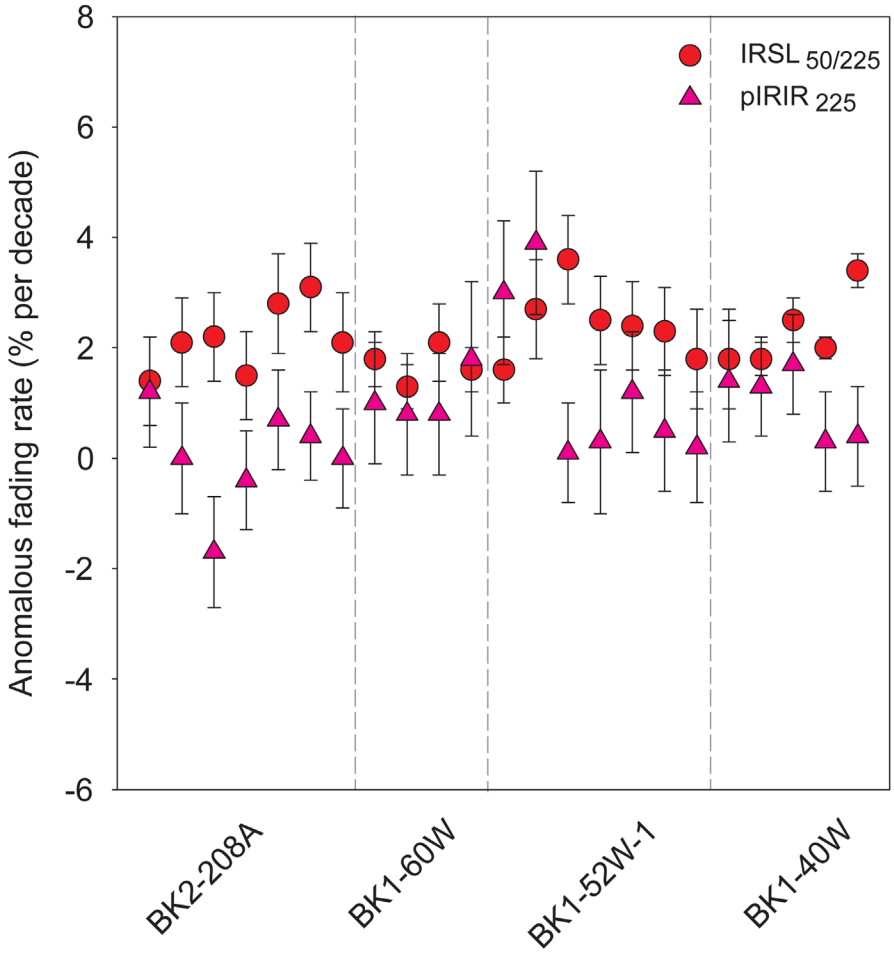


**Figure 8.** Anomalous fading test results for 23 aliquots from various BK1 core samples. Average *g*-values are 2.2% per decade for the $IRSL_{50/225}$ and 0.8% per decade for the $pIRIR_{225}$ signal.

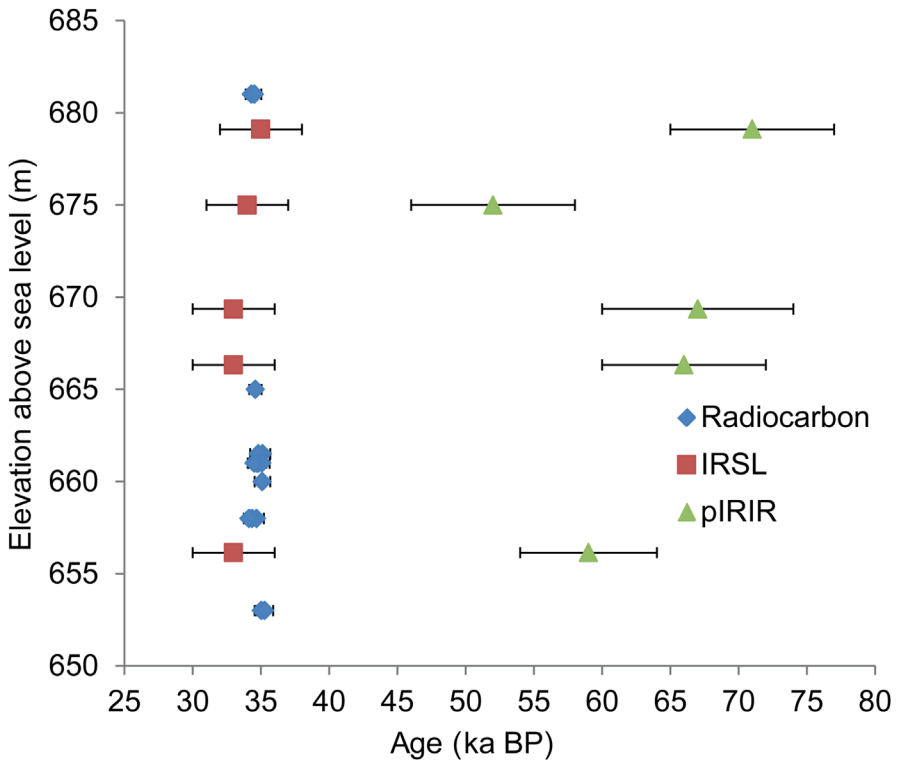


**Figure 9.** Comparison of $IRSL_{50/225}$ and $pIRIR_{225}$ derived ages with the independent radiocarbon chronology. Calibrated radiocarbon ages after Spötl *et al.* (2013) include 2σ uncertainties.

and the youngest ages of around 35 ka situated at the top of the sequence (Table 2, Figs. 3 and S3). The 98-ka age at 547.5 m a.s.l. (sample BK3-87W, see Table 2) is regarded as an outlier and not shown in Fig. 3. This sample was the only one where several dropstones were embedded in the laminated silt. This suggests a short transportation distance in a glaciolacustrine environment and, as a consequence, incomplete bleaching of the sample material. Below the IRD layer situated around 550 m a.s.l., the ages have a relatively tight distribution around 64 ka, with six out of nine ages being the same within uncertainties. Above the IRD layer, between 547 and 720 m a.s.l., there is a second cluster centred around 38 ka, but with a larger scatter and some minor age reversals. At the bottom of the drilled sequence, at ca. 475 m a.s.l., an infinite radiocarbon age of >56.3 ka BP produced from a piece of wood (measured in duplicate; 14CHRONO laboratory, Queen's University Belfast) generally supports the luminescence ages. While the scientific drill cores were sampled systematically for luminescence dating, sampling of the outcrops and BEG cores concentrated on a small number of selected locations where a clear stratigraphic connection with the lake sediments could be identified based on geomorphological and sedimentological information. These contain fine-grained (Absam, Schotterwerk III and BEG core KB-2/95, see Table 2) and coarse-grained (Bärenbach, see Table S2) sediments. The fine-grained samples from both the Schotterwerk III outcrop and BEG core KB-2/95 are consistent with the younger drill core samples and indicate sedimentation during the same time period. The three samples from Bärenbach were taken from a massive and homogeneous sand layer and yielded ages of around 54–51 ka (Table S2). With respect to age and elevation they can be connected with the lower and older ages in drill cores BK1 and BK3.

## Discussion

### *Chronology*

The relatively high $D_e$ values of the pIRIR signal (Fig. 6A) are probably the result of incomplete signal resetting before the last deposition, and therefore not suited for dating in this study. The $IRSL_{50/225}$ signal, by contrast, is considered reliable as (i) it is not significantly affected by anomalous fading and (ii) the IRSL ages agree well with calibrated radiocarbon data in the upper part of the sequence. These results seem rather unusual in general, but in the regional Alpine context, previous authors also report low fading of the IRSL and poor bleaching of the pIRIR signal (e.g. Starnberger *et al.*, 2013b; Lowick *et al.*, 2012, 2015; see the supplementary information for further discussion of anomalous fading in this context). However, knowledge of the nature and luminescence characteristics of different feldspars from various sites of this geologically complex mountain range is still limited and systematic and comprehensive investigations are needed in the future.

In addition to internal quality checks and favourable comparison to the radiocarbon ages, a previous luminescence study provides another opportunity for independent age control. Klasen *et al.* (2007) applied a modified SAR protocol to four samples taken between 690 and 660 m a.s.l. at the Baumkirchen outcrop. The resulting IRSL ages (UV) of 42–33 ka are slightly older than the corresponding ages presented in Table 2, but in three out of four cases the IRSL ages from Klasen *et al.* (2007) agree within uncertainties with the corresponding ages from the nearest elevation presented in this study (Table 2).

While Baumkirchen has long been considered an important late MIS 3 site and as the reference location of the Middle to Upper Würmian boundary (Chaline and Jerz, 1984), the new drilling and luminescence dates push the extent of the sequence, and thus its importance in Alpine Quaternary stratigraphy, back as far as at least early MIS 4 or late MIS 5a. Thus, the sediments represent far more than a brief lake phase at the end of MIS 3. Although there is some degree of scatter and several possible minor outliers (too old, possibly due to incomplete bleaching), the data provide a consistent and plausible chronology with no major age reversals or disturbances. Any offsets resulting from the occasional metre-scale slumping are insignificant compared to the size of the

luminescence age uncertainties. Thus, luminescence dating has successfully provided a chronological framework for the Baumkirchen sequence in the absence of other applicable methods.

## Lake Phases

The chronology appears to show a hiatus of ca. 7000–15 000 years constrained between ca. 549 and 545 m a.s.l. (Fig. 5). This is near the IRD-rich section, although the precise location and nature of the hiatus are not clear from the sediment. The lower phase (lake phase 1 – LP1) spans from ca. MIS 5a to latest MIS 4 or earliest MIS 3 (ca. 77–55 ka). This phase, extending from below 475 (and possibly further down as the base was not reached) to 545 m a.s.l., has an average (post-compaction) sedimentation rate of ca. 0.3–1 cm $a^{-1}$ depending on whether the inflection in the data around 496 m a.s.l. is a hiatus. The upper phase above the hiatus (lake phase 2 – LP2) spans mid- to late MIS 3 (ca. 45 to ca. 33 ka). This phase itself appears split into two sub-phases based on the chronology: a lower sub-phase LP2a from ca. 545 to 610 m a.s.l. with a sedimentation rate of ca. 0.5–1.5 cm $a^{-1}$ and an upper sub-phase LP2b from ca. 610 m a.s.l. to the top of the lacustrine sequence at ca. 725 m a.s.l. with a higher average sedimentation rate of >ca. 5 cm $a^{-1}$. The sedimentation rates, especially in LP2a, are significantly higher than seen in records of similar age and setting (e.g. Unterangerberg – Starnberger *et al.*, 2013a, and Les Echets – Veres *et al.*, 2009) providing the potential for very high-resolution proxy studies.

## Sediment composition

The transition from relatively high but low-variance Ca content in the lower part of the sequence to low but high-variance Ca coincides with the hiatus identified in the chronology at ca. 545 m a.s.l. and thus the boundary between the two lake phases (Fig. 3). The high-resolution XRF data also suggest that the mS-S layers in particular have a different elemental (both Ca and Si) and thus mineralogical (carbonate and silicate) composition. As the NCA make up only a minority of the potential catchment area, a shift in carbonate content may indicate a varying proportion of sediment coming from the Wipp and Stubai valleys, which contain the most significant carbonate-bearing catchments in the area. Much of the remainder of the potential catchment area, both the area of the Tux Alps directly to the south of Baumkirchen, and the Ötztal Alps upstream of Innsbruck, is carbonate free. Such changes in sediment source may be due to changes in the lake or catchment configuration, or changes in catchment processes such as the extent of glaciers.

Poscher and Lelkes-Felvári (1999) identified two sand sequences related to banded lacustrine sediments, the 'Baumkirchner sequence' above the clay pit (LP2) and the 'Fritzner sequence' at a lower elevation. Heavy-mineral analyses of the latter sands were dissimilar to the 'Baumkirchner sequence', more closely reflecting a sediment source from the Inn. Whether the Fritzner sequence is related to LP1 or LP2, or is unrelated is unclear. If it is related to LP1, it suggests that LP1 is probably more locally influenced. However, it is difficult to explain a significant component of carbonate minerals in the sediment without invoking the large carbonate-bearing areas of the Wipp and Stubai valleys as sediment sources at all. By contrast, the capping sands may not be directly related to the lacustrine sediments and thus may not have the same sediment source(s).

## Palaeolake configuration

The high sedimentation rate, especially in LP2, indicates relative proximity to the sediment source, in this case glaciers from the surrounding valleys. The occasional locally derived dropstones are probably transported by rafting of shoreline material by winter lake ice or from avalanches or rock falls onto such lake ice rather than being from calving of icebergs from glaciers in nearby valleys which would provide a diverse range of lithologies. Thus, the lack of iceberg-derived dropstones (except in the IRD horizon – see below) and water-lain till indicates that glacial ice was not in contact with the lake. The variations in sedimentation rate may be due to climate or catchment configuration (e.g. the presence of upstream basins trapping sediment – e.g. Schiefer and Gilbert, 2008).

The chronology of the sequence indicates that it should span a number of climate transitions. For example, the Füramoos pollen record in the northern foreland of the Eastern Alps indicates that DO events had an impact on the Alpine climate during MIS 3 (albeit in a different sedimentary setting – Müller *et al.*, 2003). South of the Alps, the Lake Fimon pollen record also reveals a sequence of DO stadials and interstadials marked by variations in vegetation (Pini *et al.*, 2010). Other lacustrine sites such as Unterangerberg and Les Echets show major sedimentological changes in response to climate shifts during this time interval. Given this, the uniformity of the Baumkirchen sequence indicates that its sedimentation regime was rather insensitive to climatic and environmental changes. This also suggests a relatively large lake which is better able to buffer the impacts of such changes. While sedimentation may also be insensitive to lake level changes, van Husen (1983b) interpreted the uniformity of the part of the sequence exposed in the clay pit as evidence of a constant rise in lake level due to constantly growing alluvial fans resulting in a near-constant water depth through time. van Husen (1983a) also linked this process to climate, suggesting increased alluvial fan growth during cooler periods. If the uniformity and high sedimentation rate of the whole of LP2b are interpreted in this way, cool climate prevailed for at least 12 000 years, requiring damming fans to aggrade in the order of ca. 170 m vertically. Given the insensitivity of the sedimentation to external factors, this need not be the case, especially as such a long-term steady climate during MIS 3 did not occur. Thus, the lake may have been dammed by alluvial fans with aggradation during cooler periods being sufficient to prevent the lake from completely filling during warmer periods with slower aggradation. It is also possible that the lake was not dammed by alluvial fans but by a larger single dam downstream (probably at the confluence of the Inn and Ziller valleys). While lake level may also be related to climate in such a scenario, this would probably result in a single large lake rather than a series of small ones between alluvial fans, and this large size would aid in buffering the deposition of sediment at the Baumkirchen site from changing climatic and environmental conditions.

## IRD and an MIS 4 ice advance

The hiatus between the two lake phases occurs near the chaotic section of unlaminated silts and clays, massive sand and matrix-supported gravel (Fig. 5). The presence of (weakly) laminated silts containing matrix-supported coarse sand-sized clasts among gravel and dropstone layers precludes debris flows as an explanation for this part of the sequence. The occurrence of angular pebble-sized clasts of distant origin embedded in a clayey silt matrix strongly suggests transport by ice rafting. This contrasts with the gravels from Schotterwerk III whose local origin and higher degree of rounded quartz-phyllite and other diagnostic cobbles indicate

fluvial transport from a local source to the south. The exotic components of the IRD layer exclude the possibility of transport by seasonal lake ice from winter avalanches or rafting of shoreline material. Rather, the pebbles are most likely transported by glaciers from the Stubai Alps to the south-west of Baumkirchen.

The highest and youngest two dates from LP1 occur within the IRD, indicating that the IRD at least partially, if not completely, belongs to LP1, putting its time of deposition around 55–60 ka. These dates demonstrate the presence of glaciers in the vicinity of the Inn Valley lake around the end of MIS 4. The presence of both fully and incompletely bleached luminescence samples within the IRD may indicate a change in conditions, the sufficiently bleached sample indicating the lake was not covered with permanent ice at the time, and the incompletely bleached sample indicating a short transport distance for the sediment in light (e.g. englacial transport and calving). The uninterrupted LP1 lake sequence indicates ice-free conditions during MIS 4 and thus only an advance at the MIS 4 to 3 transition. The lack of IRD in coeval lake sediments from the Inn Valley downstream at Unterangerberg (Starnberger *et al.*, 2013b) indicates that this glacial advance only reached the central Inn Valley.

The presence of ice provides a possible explanation for the hiatus between LP1 and LP2. Although there has been little work on Alpine subglacial lakes, the presence of even large ice sheets over lakes appears to be no barrier to sedimentation (e.g. McCabe and Ó Cofaigh, 1994; Munro-Stasiuk, 2003; Christoffersen *et al.*, 2008). Furthermore, Livingstone *et al.* (2015) recognized the difficulty in distinguishing pro- and subglacial lake sediments and given that the glacier certainly did not extend far beyond Baumkirchen, the lake would have been 'only just' subglacial; thus there is no expectation that a glacial advance over the lake would greatly inhibit sedimentation. Alternatively, a glacial advance may displace the lake water and scour the lake floor. However, as the end of the hiatus is constrained to mid-MIS 3 (ca. 42 ka), such a glacial advance causing an erosional hiatus would not be the same glacial advance which deposited the IRD at the MIS 4 to 3 transition. Furthermore, such an advance would imply a larger ice advance in mid-MIS 3 than the relatively minor one which occurred at the MIS 4 to 3 transition, which is not concordant with the pollen record from Unterangerberg which indicated less severe stadials during early to mid-MIS 3 (Starnberger et al., 2013a). Thus, the glacial advance at the MIS 4 to 3 transition does not explain the hiatus, and a later erosive ice advance in mid-MIS 3 is unlikely.

## *A sedimentation model for the central Inn Valley*

While the luminescence dates from the Baumkirchen sequence allow the identification and dating of two lake sequences, other sediments in the Gnadenwald terrace allow the formulation of a sedimentary model which puts the lake sequences in context and explains the pattern of sediments observed in the valley. The oldest dates are found in the Baumkirchen drill cores in LP1, and thus the sedimentation history begins with an initial lake sequence (LP1) at the latest during late MIS 5 and MIS 4, possibly continuing into early MIS 3 (Fig. 10 part A). While undated, silty and sandy sediments in nearby BEG cores are interpreted as belonging to the same lake phase, as younger silty sediments exist above them separated by alluvial gravels. These presumably contemporaneous lake sediments appear to coarsen upward into sands and alluvial gravels indicating basin filling with a palaeo-lake level of between 600 and 650 m a.s.l. (Fig. 10 part B).

With the possibility of a glacial origin of the hiatus excluded, the easiest way to explain either a break in sedimentation or a period of erosion is to lower the lake level or to drain the lake entirely. The absence of any coarsening-upwards sequence (e.g. the presence of deltaic sands) at the top of LP1 precludes lake filling as the reason for the hiatus. The sediments of LP2 at other nearby sites and in the BEG cores (Fig. 10 part D) appear to rest upon a steep older surface at widely different elevations, suggesting the flooding of an incised palaeo-topography. Therefore, a period of incision is inferred between the two lake phases resulting in a steep topography similar to the modern one (Fig. 10 part C). The draining of the lake could have occurred either shortly after the IRD was deposited at the Baumkirchen site, with little subsequent subaerial erosion occurring, or sometime later with any intervening sediment being removed by erosion. It is plausible that the ice advance at the MIS 4 to 3 transition could have interfered with the dam, whether the dam was an alluvial fan or a large dam near the Ziller Valley's junction with the Inn Valley (which would have hosted a large glacier tongue). Alternatively, the transition to a warmer climate in early MIS 3 (as recorded locally in the Unterangerberg pollen record – Starnberger *et al.*, 2013a) may have reduced the sediment supply to alluvial fans, allowing fluvial processes to take over as proposed by van Husen (1983a).

After re-damming the lake up to at least ca. 750 m a.s.l., lacustrine sedimentation continued at the Baumkirchen site for ca. 10 000 years, the basin filled, and silty sediments were replaced first by deltaic sands and then by fluvial gravels (also observed at the nearby Absam gravel pit). Presumably contemporaneous gravels in the Mils gravel pit at the western end of the terrace are dated to latest MIS 3 (ca. 32 cal ka BP – Spötl *et al.*, 2013). This sequence was then topped by the LGM till, possibly with a minor preceding period of erosion, and then incised to the present-day topography. This hypothesis is summarized as follows and is shown with relevant sites and dates in Fig. 10:

A. During late MIS 5, MIS 4 and early MIS 3, a lake existed and was filled with sediment. A late MIS 4 ice advance deposited a distinctive layer of IRD.
B. Basin filling continued with the deposition of alluvial fan gravels.
C. A period of erosion due to lake-level lowering or complete draining commenced, causing incision of a steep topography into existing sediments.
D. The valley was re-dammed causing flooding and deposition of lacustrine sediments on the incised topography from mid- to late MIS 3.
E. This basin continued to infill with a generally coarsening-upwards sequence in late MIS 3 depositing lacustrine banded silts/clays to delta sands to fluvioglacial gravels.
F. (not pictured) This sequence underwent partial erosion followed by the deposition of basal till during the LGM.

Relating this hypothesis to the valley bottom sedimentation model proposed by van Husen (1983a, 2000), the two lake phases may indicate cooler climate conditions with a lake forming because of rapid aggradation of local alluvial fans (van Husen's Phase A). The hiatus may represent a milder period when reduced fan sediment input allowed fluvial processes to again dominate the valley (van Husen's Phase B). However, while LP1 may simply represent cool climate conditions during MIS 4, the known climate variability

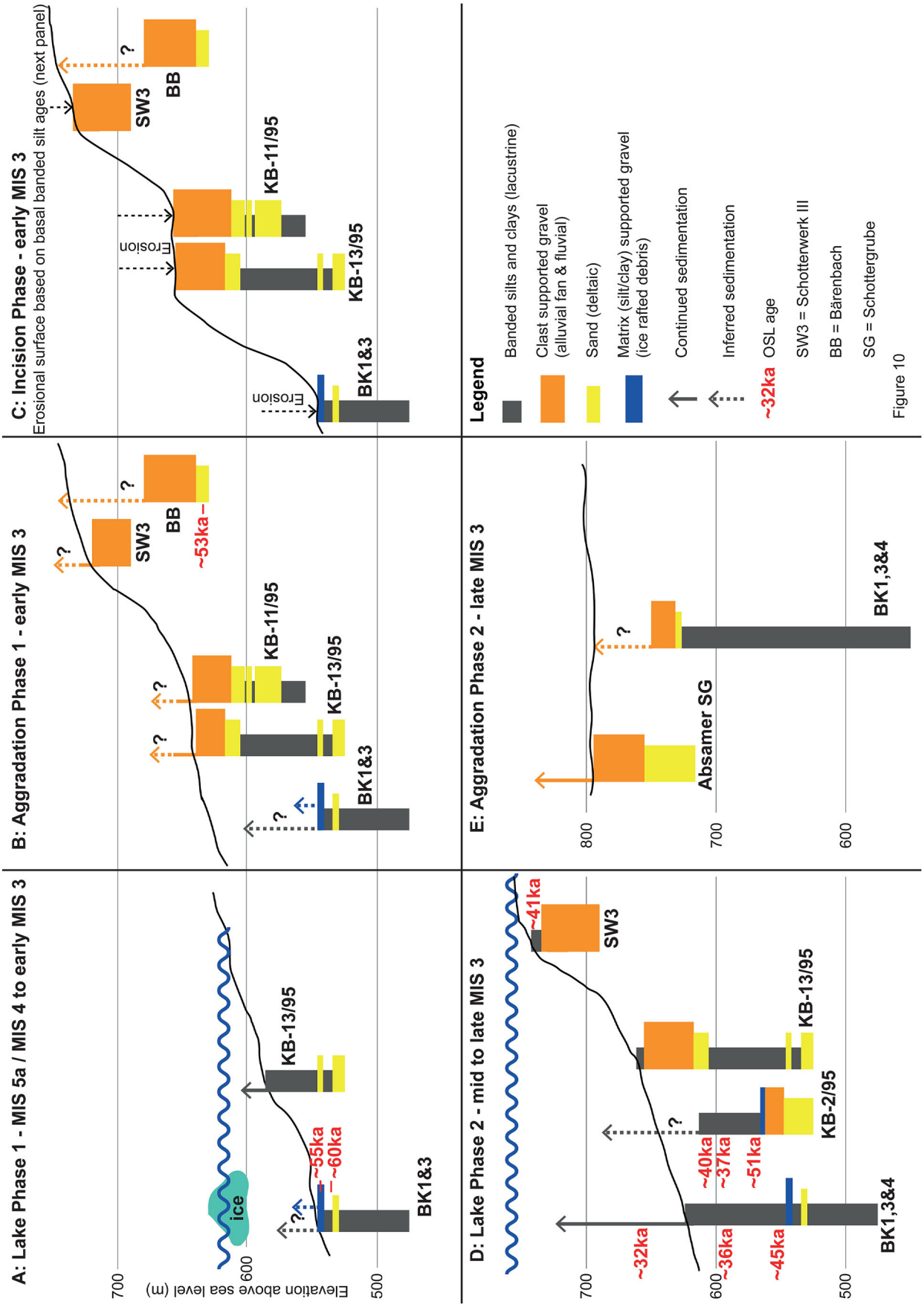


**Figure 10.** Schematic diagram of evolution of the Gnadenwald terrace showing the relevant sites and luminescence dates for each stage.

during MIS 3 precludes such a simple representation for LP2. However, the long period of lacustrine sedimentation during LP2 may have begun with a cool period when rapid alluvial fan growth caused the initial re-damming of the lake.

The question of the origin and damming of the two lake phases remains open, however. While LP1 represents a cool period and therefore fits with van Husen's Phase A hypothesis, the low elevation of the sediments allowed that basin to be potentially partially explained by glacial overdeepening, with only modest alluvial fan growth necessary to maintain lake depth. However, elevation of the upper LP2 sediments and the apparent indication of flooding of a palaeotopography preclude overdeepening as an explanation and argue for a major dam whether distant or local.

## Conclusions

New drilling has significantly extended the length of the important Baumkirchen palaeo-lake sequence. We found that the $IRSL_{50/225}$ signal from a modified IRSL SAR protocol had better bleaching characteristics and a lower residual dose than the $pIRIR_{225}$ signal. The dates derived from the $IRSL_{50/225}$ signal also matched independent radiocarbon ages for the short interval where they are available, in contrast to the $pIRIR_{225}$ ages which consistently overestimated the age. Thus, the $IRSL_{50/225}$ signal was used for dating and provides a robust chronology for the Baumkirchen sequence. This successful application of the method further demonstrates the value of IRSL dating in investigating lacustrine sediments beyond the limits of radiocarbon dating. The new dates, along with a subtle change in sediment composition identified by XRF core scanning, indicate two distinct lake phases separated by a hiatus. The earlier lake phase 1 spanned MIS 5a or early MIS 4 to late MIS 4 or early MIS 3 and is characterized by high Ca content and a low sedimentation rate and was terminated by an erosional hiatus. The later lake phase 2 spanning mid- to late MIS 3 is characterized by a lower and highly variable Ca content and a much higher sedimentation rate and was terminated by basin filling. These data, along with information from nearby outcrops and other drill cores, allowed the development of a sedimentary history model for the central Inn Valley. We discuss the possibility of different damming mechanisms for each lake phase. We also report a short section containing IRD which provides the first evidence of a late MIS 4 ice advance in the Eastern Alps. However, while ice may have just reached the central Inn Valley, it did not reach the lower valley, i.e. this ice advance was restricted to the tributaries and parts of the main valleys but did not extend to the foreland as was suggested for the Western Alps.

## Supporting information

**Figure S1.** Preheat plateau test results showing stable equivalent doses over the temperature range from ca. 220 to 280 °C.

**Figure S2.** Dose recovery test results for the IRSL and pIRIR signals from BK1 and BK3 core samples.

**Figure S3.** Stratigraphical display of (a) environmental dose rates, (b) equivalent doses (IRSL) and (c) depositional ages of the sediment samples from drill cores BK1, BK3 and BK4.

**Table S1.** Overview for dose rate-relevant data of samples from drill cores (BK1, 3, 4) and outcrops (BK00; IIIA, B; Abs 2, 3; Bae 1, 2, 3), with site name and sample code, elevation, uranium, thorium and potassium concentrations, and calculated dose rates for K-feldspar samples based on measured and estimated (25%) water content.

**Table S2.** Equivalent doses ($D_e$) and resulting ages for the central age model (CAM) applied to coarse-grained outcrop samples from the Gnadenwald terrace (n = number of aliquots; OD = overdispersion). Age models were calculated using the RLumShiny software package (www.r-luminescence.de).

*Acknowledgements.* This research was supported by the Austrian Science Fund (FWF, grant no. P24820-B16) and the Austrian Academy of Sciences (ÖAW – grant no. 23322). We are grateful to the team of Bohrgesellschaft Roßla GmbH for their excellent drilling work, Hans Peter Schuler (H. Lang Gmbh) for logistical support at the clay pit, Peter Dulski for assistance with the XRF analyses and Michael Sarnthein for his enthusiastic support during the initial phase of this project. Christoph Abfalterer helped with sieving and sorting and Peter Tropper kindly assisted in identifying rock samples. We also thank two anonymous reviewers and the editor whose comments helped to greatly improve the manuscript.

*Abbreviations.* AMS, accelerator mass spectrometry; BEG, Brenner Railway Company; BG, background; DO, Dansgaard Oeschger; ICP-MS, inductively coupled plasma mass spectrometry; IRD, ice-rafted debris; IRSL, infrared stimulated luminescence; LGM, Last Glacial Maximum; LP, lake phase; MIS, Marine Isotope Stage; mS-S, medium silt-fine sand; NCA, Northern Calcareous Alps; OSL, optically stimulated luminescence; PH, preheat; pIRIR-SAR, post-infrared stimulated single aliquot regenerative dose; XRF, X-ray fluorescence.

## References

Adamiec G, Aitken M. 1998. Dose-rate conversion factors: update. *Ancient TL* **16**: 37–50.

Aitken MJ. 1998. *An Introduction to Optical Dating*. Oxford University Press: Oxford.

Ampferer O. 1908. Über die Entstehung der Inntal-Terrassen. *Zeitschrift für Gletscherkunde* **3**: 111–142.

Anselmetti FS, Drescher-Schneider R, Furrer H *et al.* 2010. A ~180,000 years sedimentation history of a perialpine overdeepened glacial trough (Wehntal, N-Switzerland). *Swiss Journal of Geosciences* **103**: 345–361 [DOI: 10.1007/s00015-010-0041-1].

Auclair M, Lamothe M, Huot S. 2003. Measurement of anomalous fading for feldspar IRSL using SAR. *Radiation Measurements* **37**: 487–492 [DOI: 10.1016/S1350-4487(03)00018-0].

Blaas J. 1890. Erläuterungen zur geologischen Karte der diluvialen Ablagerungen in der Umgebung von Innsbruck. *Jahrbuch der Geologischen Reichsanstalt* **40**: 21–49.

Blair MW, Yukihara EG, McKeever SWS. 2005. Experiences with single-aliquot OSL procedures using coarse-grain feldspars. *Radiation Measurements* **39**: 361–374 [DOI: 10.1016/j.radmeas.2004.05.008].

Bond G, Showers W, Elliot M, *et al.* 1999. The North Atlantic's 1–2 kyr climate rhythm: relation to Heinrich Events, Dansgaard/Oeschger cycle and the Little Ice Age. In *Mechanisms of Global Climate Change at Millennial Time Scales, Geophysical Monograph Series*, vol. 112, Clark P, Webb R, Keigwin L (eds). American Geophysical Union: Washington, DC; 35–58.

Bortenschlager I, Bortenschlager S. 1978. Pollenanalytische Untersuchung am Bänderton von Baumkirchen (Inntal, Tirol). *Zeitschrift für Gletscherkunde und Glazialgeologie* **14**: 95–103.

Brauer A, Hajdas I, Blockley SPE *et al.* 2014. The importance of independent chronology in integrating records of past climate change for the 60–8 ka INTIMATE time interval. *Quaternary Science Reviews* **106**: 47–66 [DOI: 10.1016/j.quascirev.2014.07.006].

Buylaert JP, Jain M, Murray AS *et al.* 2012. A robust feldspar luminescence dating method for Middle and Late Pleistocene sediments. *Boreas* **41**: 435–451 [DOI: 10.1111/j.1502-3885.2012.00248.x].

Chaline J, Jerz H. 1984. Arbeitsergebnisse der Subkommission für Europäische Quartärstratigraphie. Stratotypen des Würm-Glazials. *Eiszeitalter und Gegenwart* **35**: 185–206.

Christoffersen P, Tulaczyk S, Wattrus NJ *et al.* 2008. Large subglacial lake beneath the Laurentide Ice Sheet inferred from sedimentary sequences. *Geology* **36**: 563–566 [DOI: 10.1130/G24628A.1].

Dehnert A, Lowick SE, Preusser F *et al.* 2012. Evolution of an overdeepened trough in the northern Alpine Foreland at Niederweningen, Switzerland. *Quaternary Science Reviews* **34**: 127–145 [DOI: 10.1016/j.quascirev.2011.12.015].

Fliri F. 1970. Neue entscheidende Radiokarbondaten zur alpinen Würmvereisung aus den Sedimenten der Inntalterrasse (Nordtirol). *Zeitschrift für Geomorphologie* **14**: 520–521.

Fliri F. 1973. Beiträge zur Geschichte der alpinen Würmvereisung: Forschungen am Bänderton von Baumkirchen (Inntal, Nordtirol). *Zeitschrift für Geomorphologie N.F* Suppl. **16**: 1–14.

Fliri F. 1975. Das Inntal-Quartär im Westteil der Gnadenwaldterrasse. *Innsbrucker Geographische Studien* **2**: 79–87.

Fliri F. 1976. Völs, Hall, Mils, Fritzens, Oelberg and further opportunities for confusing the Alpine Würm chronology. *Zeitschrift für Gletscherkunde und Glazialgeologie* **12**: 79–84.

Fliri F. 1999. *Baumkirchen. Heimatkunde eines Dorfes in Tirol*. Baumkirchen.

Fliri F, Felber H, Hilscher H. 1972. Weitere Ergebnisse der Forschung am Bänderton von Baumkirchen (Inntal, Tirol). *Zeitschrift für Gletscherkunde und Glazialgeologie* **8**: 203–213.

Fliri F, Hilscher H, Markgraf V. 1971. Weitere Untersuchungen zur Chronologie der alpinen Vereisung (Bänderton von Baumkirchen, Inntal, Nordtirol). *Zeitschrift für Gletscherkunde und Glazialgeologie* **7**: 5–24.

Frechen M, Schweitzer U, Zander A. 1996. Improvements in sample preparation for the fine grain technique. *Ancient TL* **14**: 15–17.

Heiri O, Koinig KA, Spötl C *et al.* 2014. Palaeoclimate records 60–8 ka in the Austrian and Swiss Alps and their forelands. *Quaternary Science Reviews* **106**: 186–205 [DOI: 10.1016/j.quascirev.2014.05.021].

Huntley B, Alfano MJo, Allen JRM *et al.* 2003. European vegetation during Marine Oxygen Isotope Stage-3. *Quaternary Research* **59**: 195–212 [DOI: 10.1016/S0033-5894(02)00016-9].

Ivy-Ochs S, Kerschner H, Reuther A *et al.* 2008. Chronology of the last glacial cycle in the European Alps. *Journal of Quaternary Science* **23**: 559–573 [DOI: 10.1002/jqs.1202].

Jost-Stauffer MA, Coope GR, Schlüchter C. 2005. Environmental and climatic reconstructions during Marine Oxygen Isotope Stage 3 from Gossau, Swiss Midlands, based on coleopteran assemblages. *Boreas* **34**: 53–60 [DOI: 10.1080/03009480510012836].

Klasen N, Fiebig M, Preusser F *et al.* 2007. Luminescence dating of proglacial sediments from the Eastern Alps. *Quaternary International* **164–165**: 21–32 [DOI: 10.1016/j.quaint.2006.12.003].

Köhler M, Resch W. 1973. Sedimentologische, geochemische und bodenmechanische Daten zum Bänderton von Baumkirchen (Inntal/Tirol). *Veröffentlichungen der Universität Innsbruck* **86**: 181–215.

Kulig G. 2005. *Erstellung einer Auswertesoftware zur Altersbestimmung mittels Lumineszenzverfahren unter spezieller Berücksichtigung des Einflusses radioaktiver Ungleichgewichte in der 238-U-Zerfallsreihe*. Bakkalaureusarbeit Network Computing: TU Freiberg.

Link A, Preusser F. 2005. Hinweise auf einen Vergletscherung des Kemptener Beckens (Südwest-Bayern) im Mittleren Würm. *Eiszeitalter und Gegenwart* **55**: 64–87.

Livingstone SJ, Piotrowski JA, Bateman MD *et al.* 2015. Discriminating between subglacial and proglacial lake sediments: an example from the Dänischer Wohld Peninsula, northern Germany. *Quaternary Science Reviews* **112**: 86–108 [DOI: 10.1016/j.quascirev.2015.01.030].

Lowick SE, Buechi MW, Gaar D *et al.* 2015. Luminescence dating of Middle Pleistocene proglacial deposits from northern Switzerland: methodological aspects and stratigraphical conclusions. *Boreas* **44**: 459–482 [DOI: 10.1111/bor.12114].

Lowick SE, Preusser F. 2011. Investigating age underestimation in the high dose region of optically stimulated luminescence using fine grain quartz. *Quaternary Geochronology* **6**: 33–41 [DOI: 10.1016/j.quageo.2010.08.001].

Lowick SE, Trauerstein M, Preusser F. 2012. Testing the application of post-IR IRSL dating to fine grain waterlain sediments. *Quaternary Geochronology* **8**: 33–40 [DOI: 10.1016/j.quageo.2011.12.003].

McCabe AM, Ó Cofaigh C. 1994. Sedimentation in a subglacial lake, Enniskerry, eastern Ireland. *Sedimentary Geology* **91**: 57–95 [DOI: 10.1016/0037-0738(94)90123-6].

Moseley GE, Spötl C, Svensson A *et al.* 2014. Multi-speleothem record reveals tightly coupled climate between central Europe and Greenland during Marine Isotope Stage 3. *Geology* **42**: 1043–1046 [DOI: 10.1130/G36063.1].

Müller UC, Pross J, Bibus E. 2003. Vegetation response to rapid climate change in central europe during the past 140,000 yr based on evidence from the Füramoos pollen record. *Quaternary Research* **59**: 235–245 [DOI: 10.1016/S0033-5894(03)00005-X].

Munro-Stasiuk MJ. 2003. Subglacial Lake McGregor, south-central Alberta, Canada. *Sedimentary Geology* **160**: 325–350 [DOI: 10.1016/S0037-0738(03)00090-3].

Murray AS, Wintle AG. 2003. The single aliquot regenerative dose protocol: potential for improvements in reliability. *Radiation Measurements* **37**: 377–381 [DOI: 10.1016/S1350-4487(03)00053-2].

North Greenland Ice Core Project members. 2004. High-resolution record of Northern Hemisphere climate extending into the last interglacial period. *Nature* **431**: 147–151 [DOI: 10.1038/nature02805] [Pubmed:15356621].

Penck A. 1890. Die Glacialschotter in den Ostalpen. *Mitteilungen des Deutschen und Oesterreichischen Alpenvereins* **23**: 289–292.

Penck A, Brückner E. 1909. *Die Alpen im Eiszeitalter Vol. 1. Die Eiszeiten in den nördlichen Ostalpen*. Leipzig (C.H. Tauchnitz).

Pfiffner OA. 2014. *Geology of the Alps*. Wiley-Blackwell: Chichester, UK.

Pini R, Ravazzi C, Reimer PJ. 2010. The vegetation and climate history of the last glacial cycle in a new pollen record from Lake Fimon (southern Alpine foreland, N-Italy). *Quaternary Science Reviews* **29**: 3115–3137 [DOI: 10.1016/j.quascirev.2010.06.040].

Poscher G, Lelkes-Felvári G. 1999. Lithofazielle und genetische Aspekte der Schwermineralführung alpiner Lockersedimente (Inntal, Tirol). *Abhandlungen der Geologischen Bundesanstalt* **56**: 407–414.

Prescott JR, Hutton JT. 1994. Cosmic ray contributions to dose rates for luminescence and ESR dating: large depths and long-term time variations. *Radiation Measurements* **23**: 497–500 [DOI: 10.1016/1350-4487(94)90086-8].

Preusser F. 1999a. Lumineszenzdatierung fluvialer Sedimente – Fallbeispiele aus der Schweiz und Nordeutschland. *Kölner Forum für Geologie und Paläontologie* **3**: 1–62.

Preusser F. 1999b. Luminescence dating of fluvial sediments and overbank deposits from Gossau, Switzerland: fine grain dating. *Quaternary Science Reviews* **18**: 217–222 [DOI: 10.1016/S0277-3791(98)00054-7].

Preusser F. 2004. Towards a chronology of the Late Pleistocene in the northern Alpine Foreland. *Boreas* **33**: 195–210 [DOI: 10.1080/03009480410001271].

Preusser F, Kasper U. 2001. Comparison of dose rate determination using high-resolution gamma spectrometry and inductively coupled plasma-mass spectrometry. *Ancient TL* **19**: 19–23.

Sarnthein M, Spötl S. 2012. Speculations on the spatial setting and temporal evolution of a fjord-style lake. *EGU General Assembly Conference Abstracts* **14**: EGU2012-7139.

Schiefer E, Gilbert R. 2008. Proglacial sediment trapping in recently formed Silt Lake, upper Lillooet Valley, Coast Mountains, British Columbia. *Earth Surface Processes and Landforms* **33**: 1542–1556 [DOI: 10.1002/esp.1625].

Spötl C, Reimer PJ, Starnberger R *et al.* 2013. A new radiocarbon chronology of Baumkirchen, stratotype for the onset of the Upper Würmian in the Alps. *Journal of Quaternary Science* **28**: 552–558 [DOI: 10.1002/jqs.2645].

Spötl C, Starnberger R, Barrett S. 2014. The Quaternary of Baumkirchen (central Inn Valley, Tyrol) and its surroundings. In *From the Foreland to the Central Alps. Field Trips to Selected Sites of Quaternary Research in the Tyrolean and Bavarian Alps*, Kerschner H, Krainer K, Spötl C (eds). Geozon: Berlin; 68–80.

Starnberger R, Drescher-Schneider R, Reitner JM *et al.* 2013a. Late Pleistocene climate change and landscape dynamics in the Eastern Alps: the inner-Alpine Unterangerberg record (Austria). *Quaternary Science Reviews* **68**: 17–42 [DOI: 10.1016/j.quascirev.2013.02.008] [Pubmed:23805019].

Starnberger R, Rodnight H, Spötl C. 2013b. Luminescence dating of fine-grain lacustrine sediments from the Late Pleistocene Unterangerberg site (Tyrol, Austria). *Austrian Journal of Earth Sciences* **106**: 4–15.

Thiel C, Buylaert JP, Murray AS *et al.* 2011. Luminescence dating of the Stratzing loess profile (Austria) – testing the potential of an elevated temperature post-IR IRSL protocol. *Quaternary International* **234**: 23–31 [DOI: 10.1016/j.quaint.2010.05.018].

Thomsen KJ, Murray AS, Jain M *et al.* 2008. Laboratory fading rates of various luminescence signals from feldspar-rich sediment extracts. *Radiation Measurements* **43**: 1474–1486 [DOI: 10.1016/j.radmeas.2008.06.002].

van Husen D. 1983a. A model of valley bottom sedimentation during climatic changes in a humid alpine environment. In *Tills and Related Deposits*, Evenson EB, Schlüchter Ch, Rabassa J (eds). Balkena: Rotterdam; 341–344.

van Husen D. 1983b. General sediment development in relation to the climatic changes during Würm in the eastern Alps. In *Tills and Related Deposits*, Evenson EB, Schlüchter Ch, Rabassa J (eds). Balkena: Rotterdam; 345–349.

van Husen D. 2000. Geological processes during the Quaternary. *Mitteilungen der Österreichischen Geologischen Gesellschaft* **92**: 135–156.

Veres D, Lallier-Vergès E, Wohlfarth B *et al.* 2009. Climate-driven changes in lake conditions during late MIS 3 and MIS 2: a high-resolution geochemical record from Les Echets, France. *Boreas* **38**: 230–243 [DOI: 10.1111/j.1502-3885.2008.00066.x].

Wallinga J, Murray A, Duller G. 2000. Underestimation of equivalent dose in single-aliquot optical dating of feldspars caused by preheating. *Radiation Measurements* **32**: 691–695 [DOI: 10.1016/S1350-4487(00)00127-X].

Weltje GJ, Bloemsma MR, Tjallingii R *et al.* 2015. Prediction of geochemical composition from XRF core scanner data: a new multivariate approach including automatic selection of calibration samples and quantification of uncertainties. In *Micro-XRF Studies of Sediment Cores, Developments in Palaeoenvironmental Research*, Croudace IW, Rothwell RG (eds). Springer: Berlin; 507–534.

Weltje GJ, Tjallingii R. 2008. Calibration of XRF core scanners for quantitative geochemical logging of sediment cores: theory and application. *Earth and Planetary Science Letters* **274**: 423–438 [DOI: 10.1016/j.epsl.2008.07.054].

Wintle AG, Murray AS. 2006. A review of quartz optically stimulated luminescence characteristics and their relevance in single-aliquot regeneration dating protocols. *Radiation Measurements* **41**: 369–391 [DOI: 10.1016/j.radmeas.2005.11.001].